ANALYTICAL SIMULATION OF AN INTEGRATED LIFE SUPPORT SYSTEM

O. Karl Houck

NASA Langley Research Center
Langley Station, Hampton, Va.

Presented at the ASME Annual Aviation and Space Division Conference

Beverly Hills, California
June 16-19, 1968

ANALYTICAL SIMULATION OF AN INTEGRATED LIFE SUPPORT SYSTEM

O. Karl Houck
NASA Langley Research Center

ABSTRACT

A digital computer program which solves thermodynamic-chemical equilibriums of an Integrated Life Support System (ILSS) is discussed and the system, which it simulates, is described. Comparisons of ILSS test results with various simulation cases are made. Analytical trade-off studies for spacecraft atmosphere temperature and oxygen recovery are presented. Studies that have been made are fairly accurate and provide substantiation to life support research.

INTRODUCTION

Within the past few decades, high-speed electronic computers have been utilized in many fields. The physical sciences, in particular, have largely been dependent upon the digital computer. Indeed, the assimilation of vast amounts of information generated from the space program could not be possible without the high-speed computation ability of the digital computer. In addition to processing voluminous data, two other types of physical science problems of special interest to the engineering community are efficiently solved with the aid of the computer. These are: (1) solving complex mathematical expressions that require numerical approximations; and (2) solving interrelated equations that simulate physical phenomena. Typical of the latter problem are simulation studies that involve the formulation of mathematical models which solve equations representing the physical state. The physicochemical processes of a life support system have been simulated in this manner with a generalized digital computer mathematical model developed by the McDonnell-Douglas Aircraft Corporation under contract NAS1-6448.

As the name implies, a life support system controls the mass and energy balances that are necessary to maintain a habitable environment. Analytical simulation of such a system is possible through the development of mass and energy balance relationships constrained by the physical configuration and operational characteristics of the system being simulated. Simultaneous equations could be derived from these relationships, and appropriate mathematical techniques could be applied to solve them; or, the individual relationships could be solved by iteration until system constraints have been satisfied. The latter solution concept can be more readily generalized for computer application than the former. Generalization allows simulation of virtually an endless number of possible life support system configurations. Consequently, the iterative concept was adopted to formulate computer logic of the life support system mathematical model which is described in this paper.

Although the math model has successfully been used to simulate a number of life support systems, a single application is discussed in this paper - the analytical simulation of the NASA Langley Research Center Integrated Life Support System (ILSS). The ILSS, a four-man crew regenerative system (except nutrition) built into a cylindrical test chamber with "living" and "laboratory" levels, is designed for 1 year's operation with 90-day resupply. The system is currently undergoing extensive experimental evaluations. Computer studies of the ILSS are being undertaken to complement the experimental effort and enhance the entire life support technology program at the Langley Research Center. This paper contains a brief description of the ILSS; a discussion of the computerized analytical techniques simulating the ILSS; and a presentation of some of the computer program results.

SYMBOLS

C	concentration of a particular gaseous constituent in test chamber atmosphere, pounds of constituent/pound of atmosphere
$C(0)$	concentration at some initial time $t(0)$, pounds of constituent/pound of atmosphere
$C(t)$	concentration at some instant in time t, pounds of constituent/pound of atmosphere
$\dot{m}$	mass flow rate, pounds/hour
$(\dot{m})_{CO_2}$	mass flow rate of gases or liquids as indicated by chemical formula of subscript, pounds/hour
$\dot{m}_B$	mass flow rate within "B" air conditioning subsystem, pounds/hour
$\dot{m}_C$	collection rate of water, pounds/hour
$\dot{m}_E$	actual wick evaporation rate, pounds/hour
$\dot{m}_g$	generation rate, pounds/hour
$\dot{m}_{HF}$	mass flow rate of heating fluid being transported through water recovery units, pounds/hour
$\dot{m}_{LAB}$	mass flow rate of air through laboratory area, pounds/hour
$\dot{m}_P$	required process rate of water recovery units, pounds/hour
$\dot{m}_r$	removal rate, pounds/hour
$\dot{m}_S$	wick evaporation rate for adiabatic saturation, pounds/hour
$\dot{m}_W$	mass flow rate of water vapor entering wicks, pounds/hour
$\dot{m}_1, \dot{m}_2$	mass flow rates at two different locations in cabin air circuit, pounds/hour
V	volume of ILSS test chamber, cubic feet
ϵ	effectiveness of water recovery wick (ratio of actual evaporation rate to evaporation rate at adiabatic saturation)
η_r, η_R	gas removal efficiency (ratio of removal rate to gas flow rate)
η_s	water separator efficiency (ratio of water separation rate to water flow rate)
ρ	density of test chamber atmosphere, pounds/cubic foot

γ gain factor of flow controller

NOTE: Primed quantities in text refer to re-estimated values resulting from iteration.

INTEGRATED LIFE SUPPORT SYSTEM

Figure 1 shows the regenerative processes of the ILSS. These processes are maintained by the individual subsystems identified in the figure. The integration aspects of the system are apparent when its major functions are considered.

Atmospheric condensate, urine, wash water, and CO_2 reduction product water are recovered and processed to produce potable water in the water management subsystem. Test chamber air is recirculated through charcoal filters and catalytic oxidizers for removal of contaminants. The air is cooled and dried by the air-conditioning subsystem. Moisture removed from the air is transported to the water management system. Metabolic oxygen is recovered from expired CO_2 and water vapor by physicochemical reactions occurring in the oxygen recovery subsystem. In the waste management subsystem, feces are dried and stored, and urine is piped to the water management subsystem. A bactericide is added to processed water at the personal hygiene subsystem where there are provisions for sponge bathing. Dehydrated foods are reconstituted with hot or cold processed water at the nutritional support subsystem.

Atmospheric Control

Details of subsystem functions that are germane to understanding the simulation of the subsystems will now be discussed. Subsystem orientation is shown in figure 2.

Thermal.- A conventional type of air-conditioner is used to control humidity and temperature in the test chamber. The air-conditioning subsystem has two heat exchangers, designated "A" and "B" systems, and air circulation loops. The "A" system removes humidity condensate to maintain the test chamber relative humidity between 40 and 60 percent. A propylene glycol-water solution is the cooling medium circulated through both exchangers. Test chamber temperature is kept at about 74° by the air-conditioning subsystem. Heat removed by the subsystem has varied from 25,000 to 33,000 Btu/hr during ILSS operation. Approximately 5,500 Btu/hr of this total load, produced by circulation fans, etc., has occurred within thermal control system ducting.

Contaminant.- Contaminants which must be removed include dust particles, micro-organisms, and toxic gases appearing in trace concentrations. Effective control of contaminants is obtained with particulate, bacteriological, and charcoal filters and two catalytic oxidizers. These devices are mounted within the air-conditioning ducting or receive air directly from an air-conditioner circulating fan. Electrical heaters are in the oxidizers and heat incoming air to about 750° F. A portion of the energy required to elevate the air temperature is supplied by a regenerative heat exchanger. About 5 lb/hr of the hot air flows across catalyst beds upon which low molecular weight contaminant gases are oxidized to carbon dioxide and water vapor - two gases that other subsystems can successfully process. The oxidizers may operate in either parallel or series arrangements and have a separate circulating boost fan which may be used for increased contaminant removal.

Water Recovery

Two separate identical thermodynamic loops are provided to process waste waters - urine, wash water, humidity condensate, and CO_2 reduction product water. In these loops, the waste waters are metered into a wicking material, and are evaporated leaving solid chemical contaminants within the material. The wick and other components of the evaporation circuit are shown in figure 3. Air and water vapor are circulated through the circuit by a vane-axial fan at a rate of about 40 cfm. The capacity of the airstream to evaporate water vapor is increased by elevating its temperature in the counterflow liquid-to-air heat exchanger. Water vapors are added to the airstream from the rayon felt wick which is full of waste waters and entrapped impurities. The evaporation occurring in the wick package cools the airstream to a temperature close to saturation. Airstream passage through a charcoal filter removes other impurities still vapor bound. A condenser-heat exchanger removes heat from the airstream, reducing the airstream temperature to a level somewhat below its dewpoint, thus causing condensation. Water droplets entrained in the airstream are diverted to a processed water holding tank by the centrifugal air-water separator, and the airstream passes back to the fan. One of the evaporation circuits processes about 1.2 pounds of urine per hour. The other circuit processes approximately 2 pounds of humidity condensate and wash water per hour[1]. The circuits are only operated twelve and sixteen hours each day, respectively.

Oxygen Recovery

Three units are used in recovering metabolic oxygen from expired carbon dioxide and water vapor. The arrangement and daily process rates of the subsystems are given in figure 4.

CO_2 concentration unit.- Carbon dioxide is removed from the test chamber atmosphere by thermochemical processes taking place in the CO_2 concentrator which is pictured in figure 5. Two molecular sieve bed types, silica gel and zeolite, are housed in the concentrator to adsorb water vapor and carbon dioxide, respectively. There are two each of the bed types allowing simultaneous adsorption and desorption for continuous CO_2 removal. Carbon dioxide concentration in the test chamber is maintained at about 0.7 percent (volumetric) as the concentrator removes, depending upon metabolic rates, approximately 9.28 pounds of CO_2 per day[1]. An accumulator is provided to store the CO_2 gas for later use in the CO_2 reduction unit and/or venting overboard.

CO_2 reduction unit.- There are two different modes of operation possible in the CO_2 reduction unit: (1) Bosch and (2) Sabatier. In the Bosch mode, carbon dioxide is reacted with hydrogen at about 1,200° F in the presence of an iron catalyst, producing water for oxygen recovery by electrolysis and amorphous carbon. A lower temperature reaction, 500° F, is possible in the Sabatier mode whose reaction products are methane gas and water. Unusable reaction products, carbon or methane, are stored or vented overboard, respectively. Although plagued with a number of development problems (i.e., carbon transport and removal), the Bosch mode provides a better life support materials balance. Approximately 0.84 pound hydrogen and 9.28 pounds CO_2 are combined daily in the Bosch reactor to produce 7.6 pounds of water[1].

Electrolysis unit.- The final process in oxygen regeneration is the electrolytic decomposition of water into oxygen and hydrogen. This process is performed by an ion-exchange, membrane-type, water electrolysis unit that is shown in figure 6. There are three separate modules in the unit. Each module has 16 separate cells nomially operating at about 1.7 to 2.0 volts each(1). A 25-percent sulfuric acid-water solution electrolyte is used in the unit, and it is kept at about 90° F by passing a cooling fluid through the cell stacks(1). Daily oxygen requirements for a four-man crew, 8 pounds of oxygen, are generated by the electrolysis unit(1). A portion of the required water for electrolysis, 1.4 lb/day, is obtained from the air-conditioning subsystem. The hydrogen gas generated is piped to the CO_2 reduction unit to complete the oxygen recovery cycle.

Heat Addition and Rejection

Hot and cold fluids are circulated through most of the subsystems to provide thermal energy and heat rejection. Equipment for circulating the fluids is remote from the test chamber. The heating fluid, a silicon-base oil, enters the test chamber at a temperature about 375° F, and is circulated at a rate of 300 lb/hr. A 25-percent propylene glycol water mixture, cooled to about 32° F and circulated at a rate of 1,200 to 1,600 lb/hr, satisfies heat rejection requirements.

Food, Personal Hygiene, and Waste Management

Three other subsystems, nutritional support, personal hygiene, and waste management, are in the ILSS and are intermittently operated. These subsystems, except for urine transportation from the waste management subsystem to the water recovery subsystem, and the water balance of the other two subsystems, are not part of regenerative processes. For this reason, their operation is not simulated other than heat transfer and water balance effects.

GENERALIZED LIFE SUPPORT SYSTEM COMPUTER PROGRAM

Development of the generalized life support simulation computer program has required about 6 years. Further development is still taking place. An intermediate version of the program is discussed in this paper. Computation of both steady state and transient, heat transfer, mass transfer, chemical reactions, component weight estimations, and pressure drop-flow balances for up to 90 different life support system components are possible with this version. A diagram of the program is shown in figure 7. The program has three main sections: (1) input, (2) master control block, and (3) component subroutines.

Input

In the input section, all of the information required to simulate a specific life support system is examined for possible coding errors and is filed in matrices for later use. Input information consists of program execution instructions as well as life support design and/or performance data.

Master Control Block

The master control block (MCB) performs an information management function. Instructions and data for each life support component are removed from input matrices and placed in other matrices to enable life support component simulation by the subroutines. Performance maps and/or graphical design information of components are interpolated by the MCB. A variety of tests may be performed by the MCB - for instance, comparisons of computed values with target or design goals. There are 17 different polynomial expressions of the general form $V = f(y_1, y_2, y_3, \ldots, y_n)$, $1 < n < 12$, contained in the MCB. These may be used to simulate components whose performance can be represented by a mathematical expression, such as the mathematical representation of the Stefan-Boltzmann law for radiative heat transfer. Logic is also available to permit changing input instructions during a computer run. Furthermore, control of results printout takes place in the MCB.

Subroutines

Performance of life support system components is simulated within subroutines. Physical equations applicable to the various types of life support components are in each subroutine. Thus, whenever the MCB directs problem solution to a subroutine, calculations are made to provide temperatures of working fluids exiting from the component; heat transfer to or from the component; working fluid constituent mass flow rates through the component; and estimated component weight and pressure drop across the component. Of course, these results are dependent upon input information given to the program. The simulation of the ILSS, however, is made without inputting weight and pressure drop information, so no calculations are made for these parameters. Also, each subroutine has computation options which are controlled by input instructions.

Equations

Equations used to compute life support processes can be thought of as comprising a set of linear and nonlinear algebraic equations. Two different sets of equations are used to enable the solution of steady-state and transient problems. For either of the problems, equations are solved individually rather than simultaneously. Solution to the steady-state equations is based upon latest calculated independent variables producing revised values for dependent variables until preselected convergence criteria are satisfied. Solution methodology for transient equations differs in that a noniterative technique is employed. Finite difference equations are used for transient problems. These are actually approximations to the solutions of differential equations which describe the transient behavior of individual system components. Because of the many nonlinear terms and rather arbitrary system driving functions, analytical solutions of the differential equations are generally impossible. The technique for solving the finite difference approximation equations is referred to as a forward difference or an explicit method. This technique involves imposing thermal driving conditions prevailing at the end of computing increment Δt_i to obtain new component outlet temperatures at the end of the next computing time increment Δt_{i+1}.

SIMULATION OF THE INTEGRATED LIFE SUPPORT SYSTEM

The simulation models for the ILSS consists of two individual computer programs, each of which performs different simulation tasks. Combination of the programs is possible but requires excessive computer storage that causes a longer turnaround time between runs for most computer installations. The simulation tasks of the two programs are:

(1) Steady-state analysis of the cabin air circuit;

(2) Steady-state analysis of the oxygen recovery circuit; and

(3) Transient thermal analysis of the cabin air circuit.

Generally speaking, the simulation models can be thought of as being predominantly thermodynamic systems having a number of working fluids (e.g., air, heating fluid, cooling fluid) that transfer energy within constraining boundaries through various resistance paths. Most of the paths are those between working fluids in heat exchangers and between the system and the test chamber atmosphere. The amount of energy being transferred across a boundary is proportional to the size or magnitude of the resistance path.

Input Information

Unpublished test data from a 3-day closed-door experimental evaluation of the ILSS were used in assembling input information. These data were utilized, in particular, to estimate boundary conditions and heat-transfer paths in the two circuits simulated. A UA product, the conductance to the transfer of heat U multiplied by the surface area A, from which heat is being transferred, is used to represent heat-transfer paths. Correct UA values of heat exchangers, piping, and ducting results in computer calculated cabin air and oxygen recovery circuit temperatures that are very close to their experimental counterparts. Tables 1 and 2 show selected experimental and calculated temperatures of both circuits. In addition to UA values, other test conditions, such as test chamber atmospheric pressure, cooling and heating fluid flow rates, and temperatures entering the test chamber, are compiled as input. All of the numerical quantities which are constant input values to the models are indicated in tables 1 and 2 by asterisks.

Steady state.- The steady state is characterized by mass and thermal equilibriums. Repetitive calculations are made by the computer program until these equilibriums are obtained. Two different circuits are solved for steady-state conditions. They are: (1) cabin air and (2) oxygen recovery.

Cabin air circuit: Test chamber atmosphere thermal characteristics and certain atmospheric gases are controlled by components of the cabin air circuit which is pictured by the simplified schematic diagram of figure 8. Four separate balances are involved: (1) water, (2) carbon dioxide, (3) atmospheric contaminants, and (4) thermal. At the steady state, the generation of each mass product must equal its removal rate. This is the major premise upon which inputting instructions were derived.

Water, removed by one or both of the air-to-liquid heat exchangers in the circuit and by vapor leakage from the test chamber, is considered to be produced from seven different sources:

(1) Latent Heat of men in the living area

(2) Latent Heat of men in the laboratory area

(3) Evaporation from spillage or opened water containers in the living area

(4) Evaporation from spillage or opened water containers in the laboratory area

(5) Urine - air separator (water droplets in air stream because of inefficiency of separator)

(6) Carryover in electrolysis unit oxygen stream

(7) Catalytic Oxidizers (water vapor is a product of oxidation)

With the exception of water vapor resulting from combustion processes in catalytic oxidizers, generation rates are constant input data. No water was condensed in the "B" heat exchanger based upon averaged 3-day test data. Therefore, program options were selected to force this heat exchanger to size itself until its outlet air was slightly above the dewpoint of incoming air. The "A" heat exchanger is similarly sized until a suitable UA value is defined. During theoretical studies, the UA values thus determined are designated as "total" UA values for each heat exchanger. The exchangers are divided into a "dry" and "wet" (condensing) portion. The "dry" portion is sized as previously indicated, while the "wet" portion is the difference between the total UA and the "dry" UA. Water condensed within the heat exchangers is removed at a rate determined by

$$\left(\dot{m}_r\right)_{H_2O} = \eta_s\left(\dot{m}_c\right)_{H_2O} \tag{1}$$

(Since gravity separators are being used, η_s values approaching unity are assumed.) This removal rate is used by the water process loop such that the required water processing rate can be calculated.

Fairly extensive simulation studies involving CO_2 adsorption beds have been made, for example, by Hamilton Standard, United Aircraft Corp. However, a grossly simplified simulation is used for the ILSS. The adsorption of CO_2 is expressed as

$$\left(\dot{m}_r\right)_{CO_2} = \eta_R\left(\dot{m}_g\right)_{CO_2} \tag{2}$$

Carbon dioxide is generated from two sources: (1) expired breath of test chamber occupants, and (2) oxidation processes of the catalytic oxidizers. Computational convergence is accelerated by solving two other equations:

$$\left(\dot{m}_B\right)_{CO_2} = \frac{\left(\dot{m}_B\right)_{air}\left(\dot{m}_{lab}\right)_{CO_2}}{\left(\dot{m}_{lab}\right)_{air}} \tag{3}$$

$$\left(\dot{m}_1\right)'_{CO_2} = \left(\dot{m}_g\right)_{CO_2}\left[1 + \frac{\left(\dot{m}_1\right)_{CO_2}}{\left(\dot{m}_2\right)_{CO_2}\eta_r}\right] \tag{4}$$

Equation (3) assumes that neither heat exchanger "B" or the laboratory area of the test chamber acts as sources or sinks for carbon dioxide. Since, in the simulation model, a component upstream of the laboratory simulates the addition of CO_2 to the airstream. Therefore, the CO_2 concentration in the "B" heat exchanger flow circuit is equal to the CO_2 concentration of the airstream entering the laboratory area from the "A" heat exchanger flow circuit. Carbon dioxide mass balances through the "A" heat exchanger and CO_2 concentration unit flow circuits formed the basis of derivation for equation (4).

TABLE 1.- COMPARISON OF COMPUTER INPUT AND RESULTS

WITH 3-DAY TEST DATA FOR CABIN AIR CIRCUIT

Parameter Description	Test	Computer
Number of men in living area	2	*2
Sensible heat load of each man, Btu/hr	----------	*514
Latent heat of each man, Btu/hr	----------	*567
Number of men in lab area	2	*2
Sensible heat load of men in lab area, Btu/hr	----------	*805
Latent heat load of men in lab area, Btu/hr	----------	*1355
Total atmospheric pressure in test chamber, psia	14.7	*14.7
Total flow from cooling cart, lb/hr	1098	*1098
Total flow from heating cart, lb/hr	267	*267
Living area - temperature, °F	71.2	71.3
Relative humidity, percent	40.5	41.1
CO_2 concentration, percent	0.87	**0.209
CO concentration, ppm	25 (approx.)	**11
Methane concentration, ppm	50 (approx.)	**21
Laboratory area - temperature	74.3	76.3
Relative humidity, percent	45.2	41.1
CO_2 concentration, percent	0.87	**0.209
CO concentration, ppm	25 (approx.)	**11
Methane concentration, ppm	50 (approx.)	**21
Air-conditioner system:		
A System - airflow rate, lb/hr	932	*932
Inlet air temperature, °F	79	79.8
Outlet air temperature, °F	36.2	37
Coolant flow rate, lb/hr	406	*406
Inlet coolant temperature, °F	36.2	*36.2
Outlet coolant temperature, °F	67.3	63.1
B System - airflow rate, lb/hr	2325	*2325
Inlet air temperature, °F	81.7	80.6
Outlet air temperature, °F	52	50.6
Coolant flow rate, lb/hr	800	*800
Inlet coolant temperature, °F	52	49.9
Outlet coolant temperature, °F	71	72.2
Total test chamber thermal load, Btu/hr	26,000 (approx.)	23,400

*Constant input data.
**Does not include Bosch reactor leakage.

TABLE 2.- COMPARISON OF COMPUTER INPUT AND RESULTS

WITH 3-DAY TEST DATA FOR BOSCH REACTOR

Parameter Description	Test	Computer
Reactor control temperature, °F	1192.7	1191
Heater power, kW	0.903 (approx.)	0.82
Recycle volumetric flow, cfm	3.37	*3.37
Condensing heat exchanger -		
Inlet air temperature, °F	159.8	147
Outlet air temperature, °F	No data	30.5
Coolant flow rate, lb/hr	156	*156
Inlet coolant temperature, °F	30.5	*30.5
Outlet coolant temperature, °F	36	35.3
Compressor -		
Inlet air temperature, °F	75	65.5
Outlet air temperature, °F	150	141
Outlet pressure, psia	25.32	*25.32
Regenerative heat exchanger -		
Inlet cold air temperature, °F	No data	141
Outlet cold air temperature, °F	730.2	691
Inlet hot air temperature, °F	No data	858
Outlet hot air temperature, °F	309.2	310

*Constant input data.

The effect of CO_2 leakage from the test chamber and CO_2 generation in the catalytic oxidizers were neglected.

Contaminants in the test chamber are assumed, for the simulation models, to originate from four separate sources: (1) men and equipment in the living area, (2) men and equipment in the lab area, (3) urine-fecal collection and venting of dried wastes into the cabin air circuit, and (4) purging the Bosch reactor. Generation of contaminants from these sources is simulated by inputting a constant generation rate for each source. No matter the source, contaminants are circulated through charcoal filters and catalytic oxidizers to be removed or oxidized, respectively. Additional removal, although very small, occurs from test chamber leakage. Removal by filters is proportional to an efficiency term expressed as an input constant. Oxidation reactions of the catalytic oxidizers are based upon combustion theory using a removal efficiency, heat of combustion, and the amount of carbon (weight) in each mass weight of contaminant as input constants. This information allows a computation of carbon dioxide, heat, and water generation rates, and oxygen use rate. Contaminant levels of 250 ppm methane and 50 ppm carbon monoxide were assumed for the studies reported in this paper. Again, computational convergence is accelerated by the solution of another equation. Using the same analogy as was used for carbon dioxide balance, a trace contaminant flow rate in the "B" heat exchanger circuit can be expressed as

$$\left(\dot{m}_B\right)_{trace} = \frac{\left(\dot{m}_B\right)_{air}\left(\dot{m}_{lab}\right)_{trace}}{\left(\dot{m}_{lab}\right)_{air}} \qquad (5)$$

The thermal balance in the test chamber is the most complex and difficult balance to simulate. It includes all heat transfer between life support system components, including piping and ducting, and the test chamber atmosphere as well as heat transfer to and from airstreams by components operating in airstreams; the transfer of thermal energy through the walls of the test chamber; and the latent and sensible heat loads of test chamber occupants. At the steady state, all of the thermal energy generated in the chamber is removed by heat exchangers "A" and "B," and heat transfer through test chamber walls.

As previously noted, thermal loads and UA values were selected by trial and error until calculated system temperatures were very nearly equal to 3-day test counterparts. Table 1 lists the final thermal conditions required to produce the temperature characteristics evidenced in the table.

The water processing loops are also simulated by the cabin air circuit simulation model. The rate of evaporation in wicks is determined by

$$\left(\dot{m}_E\right)_{H_2O} = \epsilon\left[\left(\dot{m}_S\right)_{H_2O} - \left(\dot{m}_W\right)_{H_2O}\right] \qquad (6)$$

The rate at which water is removed from the loop is calculated by an equation identical to equation (1). Using the desired processing loop operating time period as input, the program determines a required processing rate from

$$\left(\dot{m}_P\right)_{H_2O} = \frac{24}{t_o}\sum_{j=1}^{N}\left[\left(\dot{m}_R\right)_{H_2O}\right]_j \qquad (7)$$

A re-estimating polynomial that simulates the action of a flow controller is used to adjust heating fluid flow until the desired process rate is realized. The polynomial has the form

$$\dot{m}'_{HF} = \dot{m}_{HF}\left\{1 - \gamma\left[\frac{\left(\dot{m}_P\right)'_{H_2O} - \left(\dot{m}_P\right)_{H_2O}}{\left(\dot{m}_P\right)_{H_2O}}\right]\right\} \qquad (8)$$

To provide room for additional components used in the studies to be described later, the water processing loop had to be removed from the simulation model, and is, consequently, not discussed further.

Oxygen recovery circuit: The Bosch reactor configuration of the oxygen recovery circuit was chosen for simulation. Figure 9 is a schematic diagram of the oxygen recovery circuit. A special subroutine was prepared for the simulation to enable analysis of gas composition at various locations in the Bosch recycle gas loop. Calculations possible for recycle gas constituents are: (1) weight fractions, (2) volume fractions, (3) partial pressures, and (4) mass flow and volumetric flow rates. Constituents of the recycle gas are assumed to be: (1) methane, (2) carbon monoxide, (3) carbon dioxide, (4) hydrogen, (5) water vapor, and (6) trace amounts of oxygen and nitrogen that appear as a result of inefficiencies of other life support processes. Other significant calculations performed by the subroutine are: (1) temperatures of flow streams; (2) effective specific heat of gas flows; and (3) heat transfer of chemical reactions.

Actual test conditions of the oxygen recovery circuit are initially simulated by the judicious selection of heat-transfer conditions in a similar manner to that used for the cabin air circuit. A comparison of test results and the simulation is made in table 2. Input information, other than heat-transfer conditions, consists primarily of initial choices for certain parameters that are later changed by successive iterations. The supply rate of carbon dioxide is recalculated as a consequence of the purge flow that rids the recycle gas loop of nitrogen and non-condensables; and the chemical reactions occurring in the Bosch reactor. Final values of electrical energy required to maintain the desired Bosch reactor temperature and recycle loop volumetric flow rate are also calculated from preselected original values. The electrical energy is changed to offset the thermal energy lost from the loop, while recycle flow is maintained close to the desired value by altering the bypass flow around the recycle compressor.

Several chemical reactions take place concurrently in the Bosch reactor. Those of major significance are:

(1) $CO_2 + 2H_2 \rightarrow C + 2H_2O$

(2) $CO_2 + 4H_2 \rightarrow CH_4 + 2H_2O$

(3) $CH_4 \rightarrow C + 2H_2$

(4) $CO_2 + H_2 \rightarrow CO + H_2O$

(5) $2CO \rightarrow CO_2 + C$

The technique of simulating the above equations is by linear interpolation of hypothetical reactor performance curves. A typical set of curves is shown in figure 10. The curves were constructed as look-alikes to chemical reaction data observed by other investigators. They generally resemble experimental data reported and provide a means of showing performance trends in the

Bosch reaction process. Ordinates in the curves relate to reactor pass efficiency, the ratio of the amount of carbon dioxide reacting to the amount being recycled. Dimensionless parameters, obtained from the ratio of recycle loop gas constituent partial pressures and the ratio of oxygen to hydrogen atoms in the recycle gas loop, are the independent variables. Values interpolated from the curves are used to determine gas constituent mass flow rate changes and reaction thermodynamics.

Oxygen recovery circuit simulation contains a computer model of the electrolysis unit which simulates the production of hydrogen and oxygen from water. Essentially, the simulation is based upon re-estimating electrical power supplied to the unit until the required hydrogen flow for the CO_2 reduction unit is achieved. Simulation studies made to date have not considered electrolysis.

Transient.- The transient simulation allows for the determination of transient thermal behavior and the transient characteristics of test chamber atmospheric constituents. Thermal transients are basically temperature lags encountered in ducting and plumbing that interconnect components. Concentrations of test chamber atmospheric constituents, oxygen, nitrogen, carbon dioxide, and trace contaminants, change slowly with respect to time as a result of the relatively large test chamber and low generation and removal rates.

Information compiled to enable steady-state solutions is also used in transient analysis. In addition, the thermal capacitance of certain components must also be specified as input data. Transient characteristics of gases are simulated by the equation

$$\rho V \frac{d}{dt} C = \dot{m}_G - \eta_R \dot{m} C \qquad (9)$$

which may be solved with calculus to yield

$$C(t) = C(0)e^{-\frac{\eta_R \dot{m}}{\rho V}(t)} + \frac{\dot{m}_G}{\eta_R \dot{m}}\left(1 - e^{-\frac{\eta_R \dot{m}}{\rho V}(t)}\right) \qquad (10)$$

An additional simulation capability, the action of controllers, is available. Types of controllers that may be simulated are: two position; proportional position; floating; proportional speed floating; derivative; and proportional plus floating. Also, the following types of feedback in addition to a single feedback loop can be simulated: input derivative; error derivative; error integral; and output derivative. Input data for this simulation are controller operational characteristics, either estimated or experimental.

Typical Results

The computer mathematical models previously described have been used to assist in studying selected ILSS performance problems. Experience has shown that the air-conditioning subsystem was not capable of maintaining comfortable conditions at certain heat loads. A modification to the existing design was developed and was analyzed during development with the simulation model. Test data from the Bosch reactor have been difficult to interpret because of carbon removal and transport problems. Analytical studies of a very preliminary nature were made to provide additional insight of Bosch reactor performance.

A basic simplifying assumption has been applied to all the studies. This assumption is that UA values are unchanged regardless of flow changes. The UA values determined from ILSS 3-day test data are used throughout the studies. This assumption appears reasonable since the local heat-transfer film coefficient only changes by a factor of 18 for two to three orders of magnitude of change in flow[2]. As a consequence, the U term, being indirectly proportional to the sum of local heat-transfer film coefficients, is not significantly changed.

Air-conditioning subsystem.- Past and present designs of the air-conditioning subsystem are illustrated in figure 11. The present design increases subsystem cooling capacity by supplying heat exchanger "B" with coolant at a lower temperature than the previous design. Three controllers for maintaining the indicated temperatures at desired control points have also been added. Relative humidity is kept within comfortable limits by the selection of the proper air balance to the living and laboratory levels from the heat exchanger "A" subsystem, and the air outlet temperature of heat exchanger "A." The effect these two parameters have on relative humidity and temperature conditions was analyzed. Also included in the analysis was a determination of coolant flow supplied to heat exchangers "A" and "B," resulting in the best combinations of test chamber thermal conditions. Since these studies assisted in the selection of coolant flow controller settings actually used, they were made for an estimated maximum test chamber heat load of 33,000 Btu/hr.[3] The flows thus determined are those which must be obtained with the controllers in a wide-open position. Nominal heat loads cause the controllers to partially close and divert some of the coolant fluid around the heat exchangers such that test chamber thermal conditions are maintained at the desired control point. Results from these studies are shown graphically in figure 12.

In figure 12(a), test chamber temperature-humidity conditions are plotted as a function of the coolant flow division between "A" and "B" heat exchangers and the airflow division to the living and laboratory levels from heat exchanger "A." Approximately 90 percent of the total heat load occurs in the laboratory level. This results in lower laboratory temperatures being realized when more "A" system flow is supplied to the laboratory level. However, if 75 percent or more of the total flow (1,428 lb/hr) passes through the laboratory, it is impossible to keep the living level temperature and heat exchanger "A" outlet air at their control points, 74° F and 40° F, respectively. The best temperature conditions are seen to take place when 35 percent of the total coolant flow (1,200 lb/hr) is made available to heat exchanger "A" and there is an equal division of "A" system air delivered to the living and laboratory levels. At these points, relative humidity is not at its most comfortable value. Some humidity control is possible by adjusting the outlet air temperature of heat exchanger "A." Figure 12(b) illustrates this.

Heat exchanger "A" air outlet temperature is one of two independent variables of figure 12(b). The other independent variable is the same as used in figure 12(a), fraction of coolant flow available to heat exchanger "A." It should also be noted that there is an equal airflow division between the living and laboratory levels from the "A" system. Outlet air temperature for this condition with a coolant flow division of 35 percent has little influence upon laboratory relative humidity and a minor effect upon living level

relative humidity. Nevertheless, an outlet air temperature of 45° F is more desirable to produce the most comfortable relative humidity. Laboratory temperature is seen to be little effected by air outlet temperature. It is again evident that the best available coolant flow setting is about 35 percent with control of living level and air outlet temperatures possible for coolant flow fractions greater than 30 percent.

Air-conditioning capacity is indicated in the curves of figure 13, that are based upon the best operational conditions, air outlet temperature of 45° F; 50/50 system "A" airflow split; and 35 percent total coolant flow to heat exchanger "A." Comfortable test chamber conditions, except humidity, can be expected for the thermal loads that have been experienced during actual ILSS operation. Thermal loading greater than 33,000 Btu/hr, which is the maximum estimated heat load, results in losing control over laboratory level temperature. Other facts worthy of mention are evident from the curves. There is sufficient heat exchanger "A" capacity, the difference between H/X "A"-coolant flow and point A on the ordinate, to enable a reduction of the air outlet temperature. Or, overall system capacity can be further increased by diverting more coolant to the "B" heat exchanger. Finally, it appears possible, because air is being bypassed around heat exchanger "A" at the highest thermal loading, to increase the living level heat load and still obtain the desired living level temperature.

Improvement of the air-conditioning design is evident when the theoretical curves are compared with test data from the older design. (The symbols shown in the figure indicate performance of the older design.) With the old design, an acceptable laboratory temperature was only possible at the indicated thermal loading with the maximum available coolant flow being circulated through the heat exchangers. Furthermore, no air was being bypassed around heat exchanger "A." No increase in heat loads beyond the average load of the test is possible with the older design.

Bosch-CO_2 reduction unit.- The primary objective of the Bosch reactor studies was to define the operational characteristics which influence water production rates and to examine the extent of their influence. A secondary objective was to determine if there are deficiences in the CO_2 reduction simulation model. The objectives were realized by independently changing the magnitude of certain operating conditions and noting their effect upon reactor performance. Conditions that were varied are: (1) flow rate of coolant fluid through the condenser; (2) volumetric flow rate in the recycle loop; (3) Bosch reactor control temperature; (4) purge flow from the recycle loop; (5) compressor outlet pressure; and (6) mixture ratio of hydrogen-carbon dioxide being supplied to the unit. Item 4 simulates, to a limited degree, recycle leakage that has been experienced during tests. Performance of the reactor may be judged by three parameters. These are: water production rate; a reaction factor; and a production factor. Water production rate is the amount of water produced on a daily basis. Chemical performance in the reactor is indicated by the reaction factor which is the ratio of the rate at which carbon dioxide is being consumed to the rate at which it is being recycled through the reactor. Overall CO_2 reduction performance is expressed with the production factor which is the ratio of water production rate to the electrical energy required to keep the reactor at the selected operating temperature. In the curves of figure 14, performance parameters are plotted against each of the independently varied test conditions. It must be kept in mind that the curves, although the result of steady-state simulation, represent relationships at a single instant of time. Should some of the selected test conditions persist over a period of time, chemical reactions would eventually cease because of the reactants not being stoichiometrically replenished. Numerical values of each operating condition determined from averaging 3-day test data are denoted. Whenever a single condition was varied, all other conditions were kept constant.

Condenser coolant flow: Variations in coolant flow rate through the condenser has no effect on performance for a flow range of about 30 percent to 250 percent of the 3-day test point, 156 lb/hr. This indicates that the condenser is adequately sized to produce the highest possible condensation rate for coolant flow rates which might be encountered during normal operation. Two other conditions, coolant inlet temperature and entrained water separation rate, effect condensation rate and thus, production rate. During actual operation these conditions are relatively invariant and were therefore not simulated.

Compressor outlet pressure: In its present form, the Bosch reactor simulation does not contain information to simulate system pressure drops although program logic is available for this simulation. Thus, pressure drop effects on performance cannot be analyzed and performance is independent of system total pressure. Problems with carbon removal and transport during tests have effected recycle gas loop pressures and have produced perturbations to water production.

Recycle flow: Water production can be altered without appreciably affecting reaction and production factors by changing recycle flow. According to the results obtained, however, it appears that there is an optimum recycle flow that yields a maximum water production rate. Reaction and production factors are seen to be relatively insensitive to recycle flow. It is expected that the gradual decrease of production factor is a result of thermal losses being directly proportional to flow. At a flow less than optimum, the rate change in water production and thermal losses are about equal.

Reactor temperature: Another inadequacy of the simulation model is evident in figure 14(d). There is no relationship between chemical reactions and reactor temperature. The figure also shows that production factor decreases at elevated temperatures because of the additional power required to maintain these temperatures.

Purge flow: Purging the Bosch reactor recycle loop is sometimes required to rid the loop of unreactive gases. Leakage from the recycle loop is also simulated with the purging capability. Because of the very small quantities of nonreactive gases used in the simulation model, only slight changes are noted in figure 14(e) as purging is stopped (i.e., purge flow approaches zero). When purging is increased beyond requirements for reaction poisoning, smaller quantities of reactants are passed through the reactor resulting in a drop-off in water production. Reaction factor is improved with leakage because the amount of carbon dioxide being recycled is decreasing at a more rapid rate than the rate of consumption. Since less power is needed for the reduced flow through the reactor, because heat losses are proportional to reactor flow, production factor increases with leakage even though water production is reduced.

Mixing ratio: The interaction of the various reaction curves in the simulation model is evident in figure 14(f). It is to be remembered, of course, that the results shown are at one instant of time. Reactions would be impossible to maintain at the hydrogen-rich mixtures shown. It is interesting to note that reactions are still taking place near a reactant mixing ratio of 1, although water production has ceased. This is attributed to poor heat-transfer characteristics of the hydrogen-rich recycle gas[4] resulting in thermal conditions that renders the condenser useless.

Test results: Recycle gas composition effects have also been noted during tests. Figure 15 is a plot of water production obtained during tests versus hydrogen-carbon dioxide volumetric concentration ratio at the reactor outlet. Various analytically derived points from previously discussed studies have been superimposed in the figure. Data points obtained from the simulation model generally produce higher production rates indicating that reaction curves of the simulation model have been optimistically constructed. It is further shown that the analytical data is without a definite trend. These characteristics are likely the result of simulation deficiencies previously noted.

CONCLUDING REMARKS

A generalized life support system computer program has been adapted to simulate operation of the Langley Research Center Integrated Life Support System. Utility of the program in this role has been demonstrated by using it to assist in solving some problems that have become evident during ILSS research. Comparison of results from computer simulation with those of actual tests have shown the simulation model can provide reasonably accurate results when simulating the cabin air circuit, but improvement is required for accurate oxygen recovery circuit simulation. Further sophistication and improvement to the model is anticipated such that it can provide additional analytical support to the NASA life support research effort. Continued use of the simulation model in conjunction with ILSS experimental evaluations is expected to produce the life support technology required for long-term orbital and interplanetary missions, and the eventual development of real-time onboard computers that will survey and control life support processes.

REFERENCES

1. Pecoraro, J. N., A. O. Pearson, G. L. Drake, and J. R. Burnett, "Contribution of a Developmental Integrated Life Support System to Aerospace Technology," AIAA 67-924, October 1967.

2. McAdams, W. H., Heat Transmission, McGraw-Hill Book Co, Inc., Third Edition, 1954.

3. Armstrong, R. C., M.D., "Life Support System for Space Flights of Extended Time Periods" - Final Report, General Dynamics - Convair, NASA-CR-614, 1966.

4. Sutton, George P., Rocket Propulsion Elements, pp. 98-99, John Wiley & Sons, Inc., Second Edition, 1957.

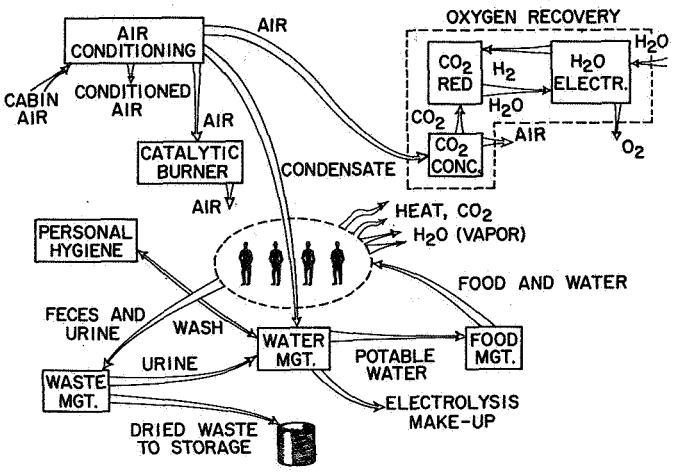

Figure 1.- ILSS regenerative processes.

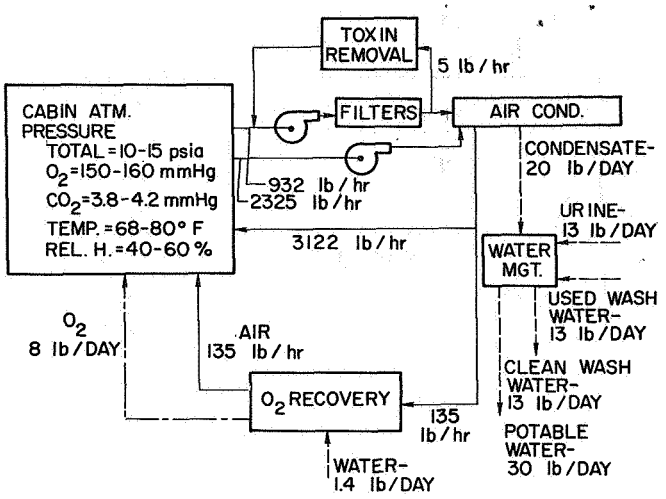

Figure 2.- Subsystem orientation.

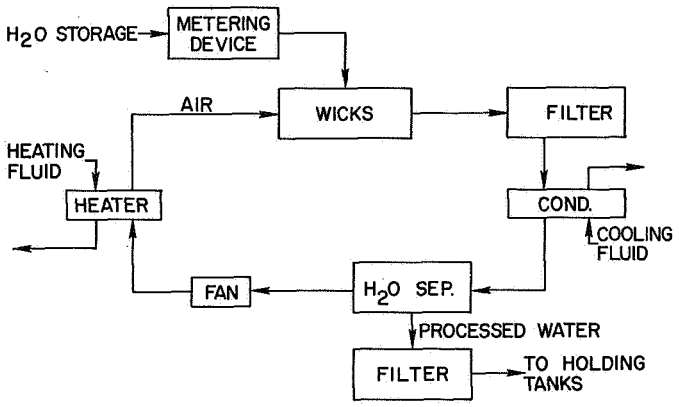

Figure 3.- Typical water processing unit.

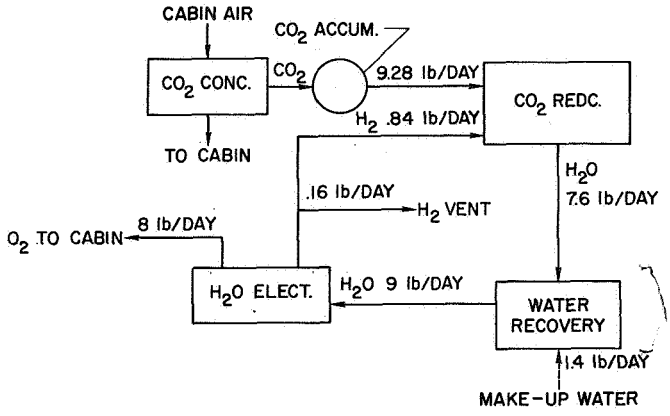

Figure 4.- Oxygen recovery subsystem.

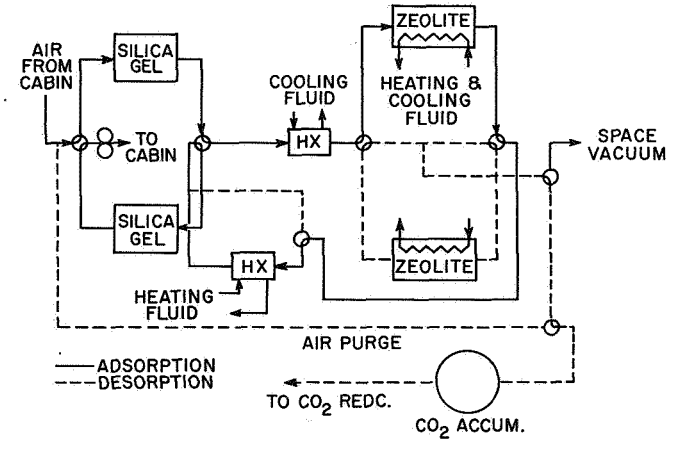

Figure 5.- CO_2 concentration unit.

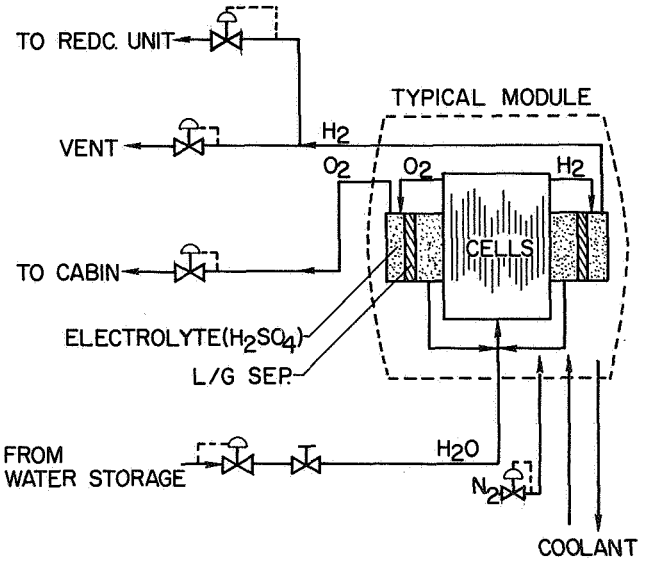

Figure 6.- Electrolysis unit - module.

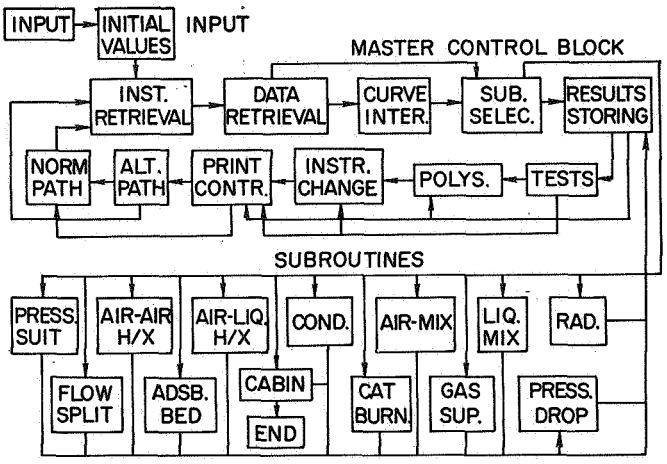

Figure 7.- Generalized life support computer program.

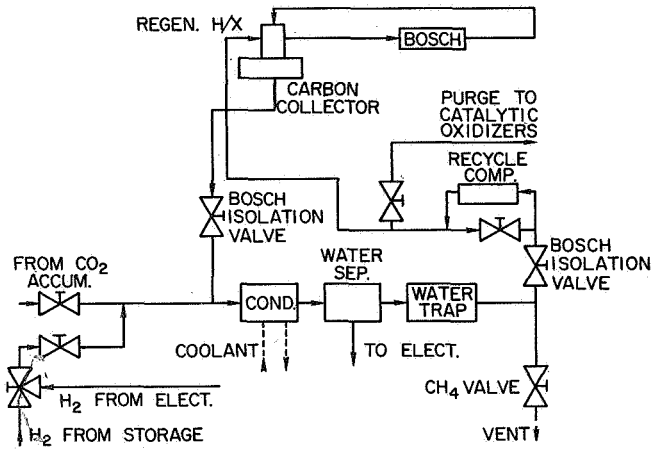

Figure 9.- Oxygen recovery circuit simulation model - Bosch reactor.

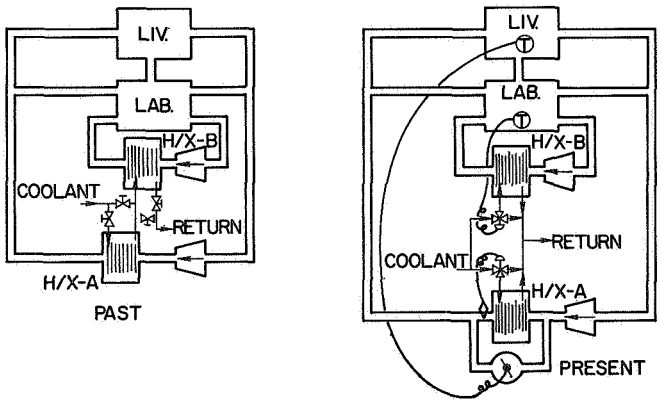

Figure 11.- ILSS air conditioning subsystem designs.

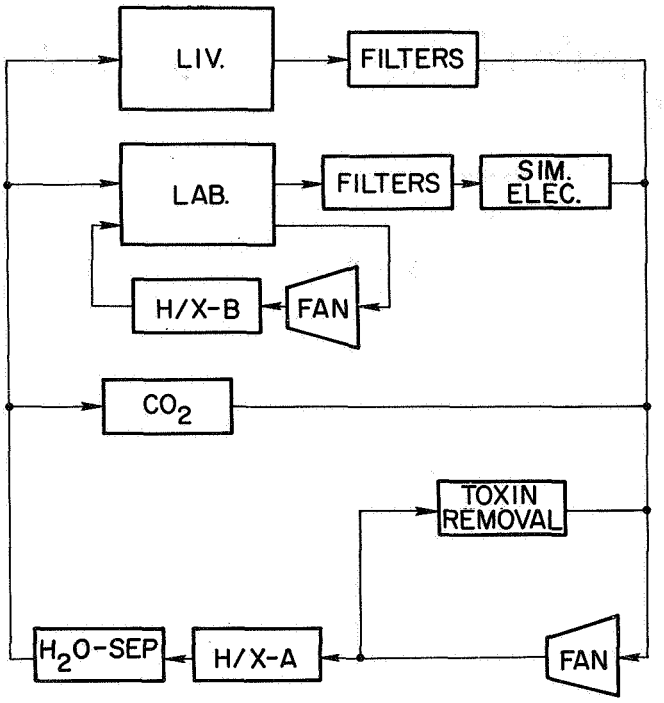

Figure 8.- Cabin air circuit simulation model (simplified).

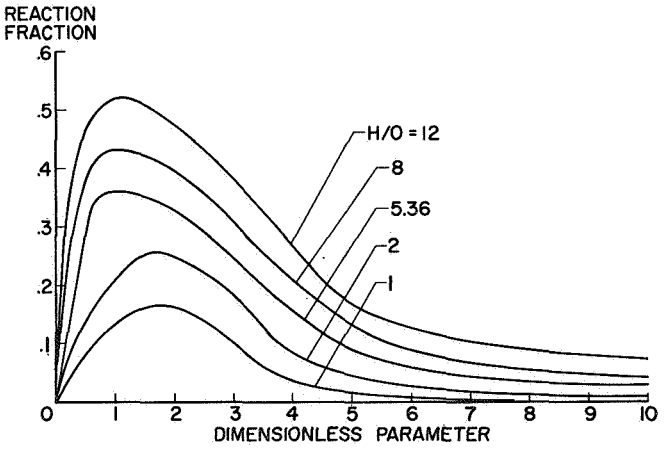

Figure 10.- Bosch reactor performance - primary reaction $CO_2 + 2H_2 \rightleftharpoons C + 2H_2O$.

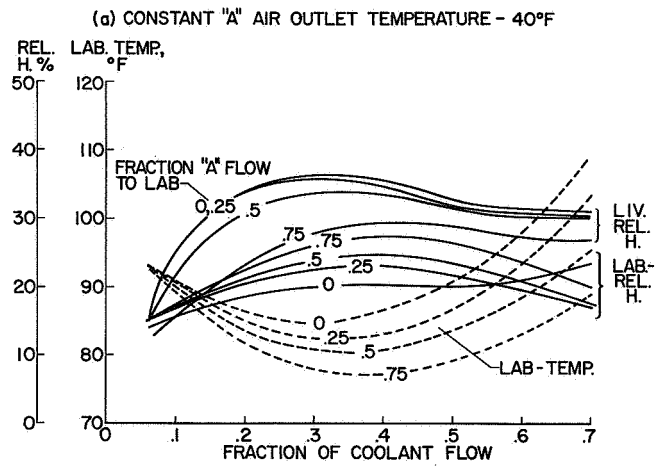

Figure 12.- ILSS air conditioning performance.

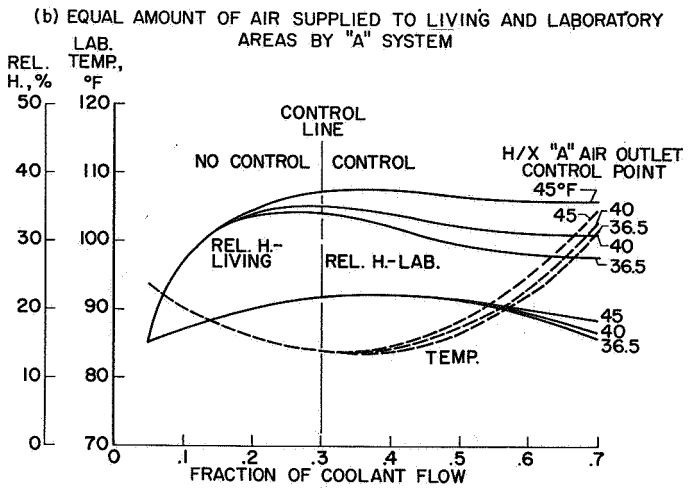

Figure 12.- Concluded.

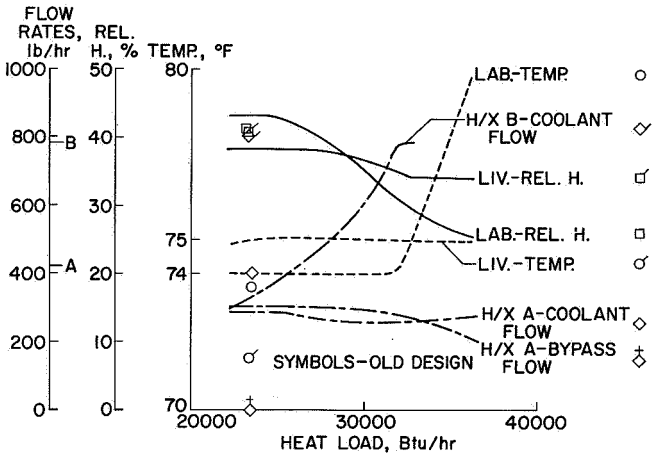

Figure 13.- Capacity of new air conditioning design.

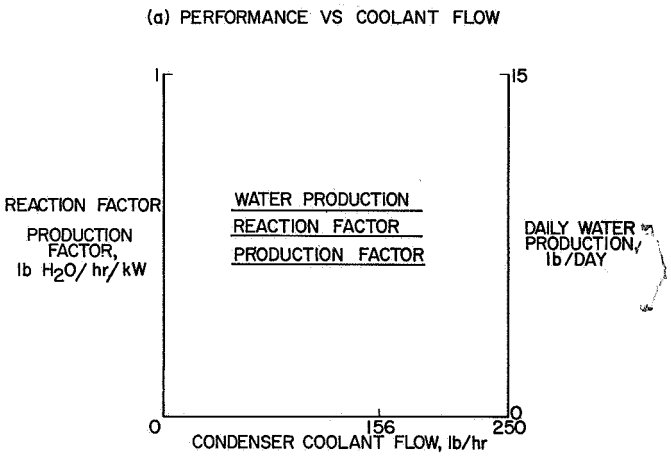

Figure 14.- Bosch reactor system performance trends.

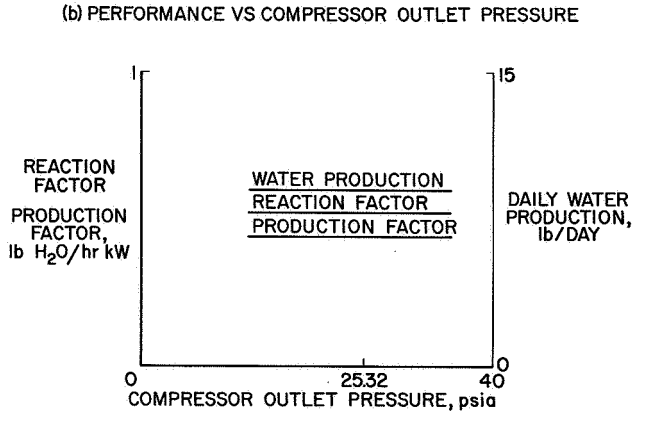

Figure 14.- Continued.

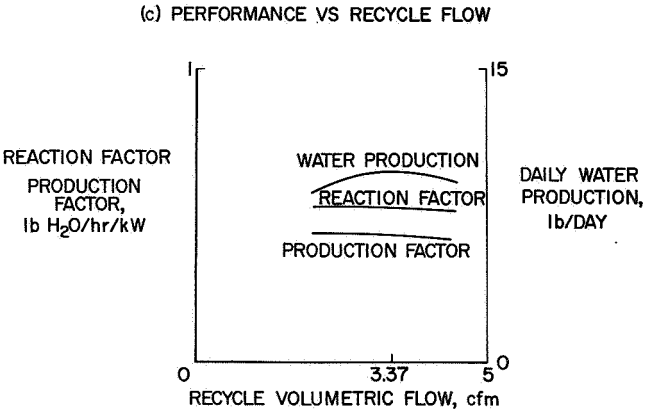

Figure 14.- Continued.

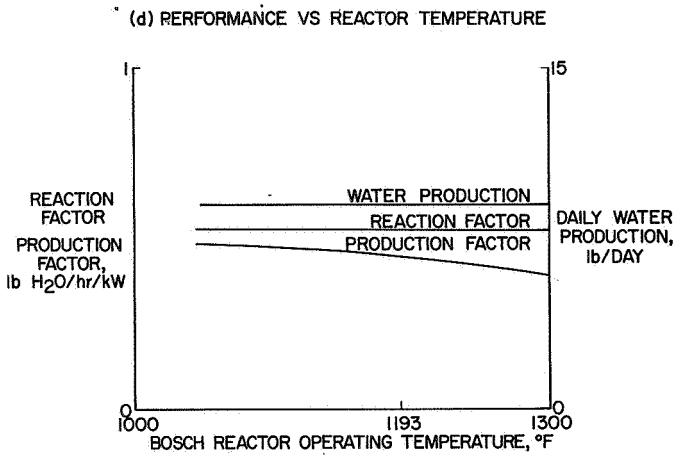

Figure 14.- Continued.

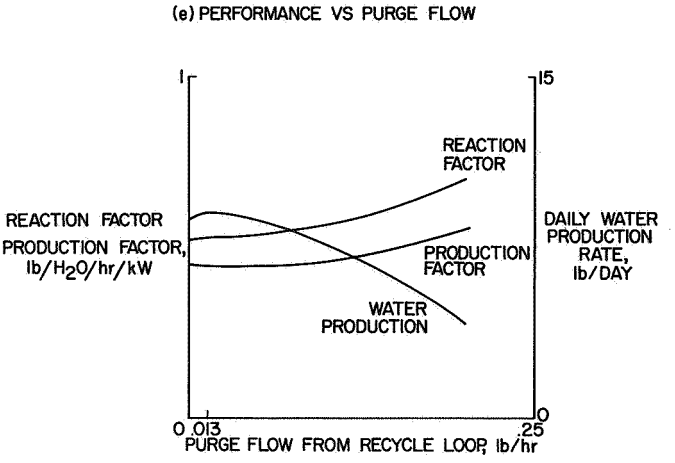

Figure 14.- Continued.

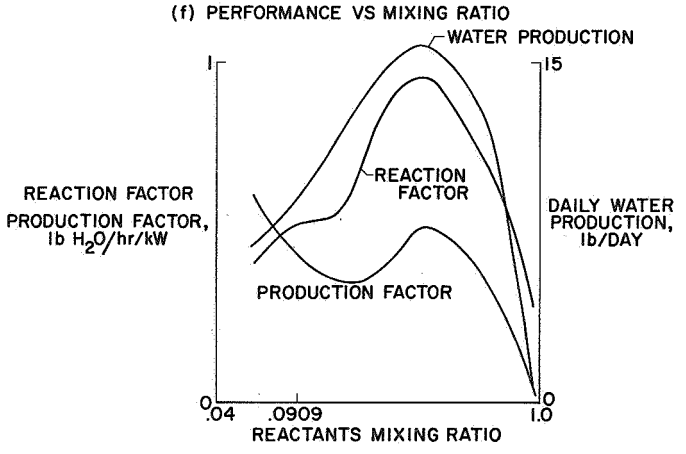

Figure 14.- Concluded.

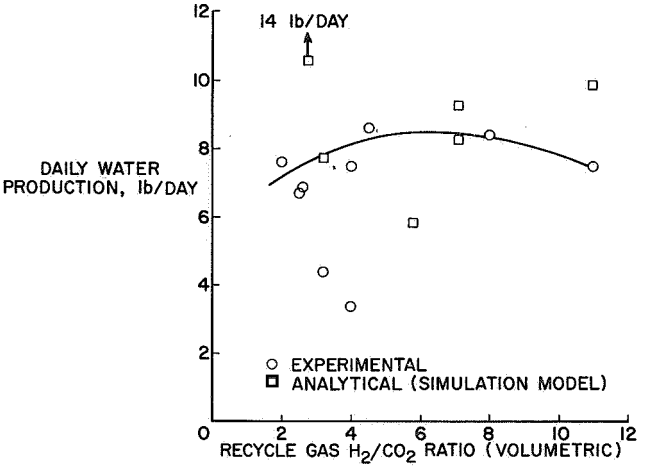

Figure 15.- Experimental and theoretical Bosch reactor performance.